NJC

Accepted Manuscript

This is an *Accepted Manuscript*, which has been through the Royal Society of Chemistry peer review process and has been accepted for publication.

Accepted Manuscripts are published online shortly after acceptance, before technical editing, formatting and proof reading. Using this free service, authors can make their results available to the community, in citable form, before we publish the edited article. We will replace this *Accepted Manuscript* with the edited and formatted *Advance Article* as soon as it is available.

You can find more information about *Accepted Manuscripts* in the Information for Authors.

Please note that technical editing may introduce minor changes to the text and/or graphics, which may alter content. The journal's standard Terms & Conditions and the Ethical guidelines still apply. In no event shall the Royal Society of Chemistry be held responsible for any errors or omissions in this *Accepted Manuscript* or any consequences arising from the use of any information it contains.

ROYAL SOCIETY OF CHEMISTRY

www.rsc.org/njc

Journal Name

RSCPublishing

ARTICLE

Synthesis of Carboxylate Functionalized A_3B and A_2B_2 Thiaporphyrins and Their Application in Dye-Sensitized Solar Cells

Cite this: DOI: 10.1039/x0xx00000x

Received 00th January 2012,
Accepted 00th January 2012

DOI: 10.1039/x0xx00000x

www.rsc.org/

Sandeep B. Mane [a, b] and Chen-Hsiung Hung[a*]

A series of novel A_3B and A_2B_2 thiaporphyrins consisting of mono or dual anchoring groups with different linkers has been synthesized and effectively applied in dye-sensitized solar cells (DSSCs). The presence of ethynylphenyl linker has pronounced effect on their optical, electrochemical and photovoltaic properties. The ethynylphenyl linker bathochromically shifted the absorption spectra. The density functional theory (DFT) studies revealed that attachment of ethynylphenyl linker through one of the *meso* position to the porphyrin core results in planar macrocycles which is essential for the active electron coupling of the porphyrin core with the anchor group in DSSCs. Although the dual anchoring groups can bind strongly to the TiO_2 surface, the presence of ethynylphenyl linker and moreover the electron withdrawing cyano group on the anchoring group proved to be the pivotal factors to achieve higher efficiency. Among these dyes, N3S-ECN having ethynylphenyl linker and a cyano acrylic acid as the anchor, achieved the highest efficiency of 1.69%, with J_{sc} = 5.12 mA cm^{-2}, V_{oc} = 0.49 V and FF = 67%. To the best of our knowledge this is the highest efficiency obtained for thiaporphyrins.

Introduction

Developing renewable energy resources to replace the depleting fossil fuel reserves is the biggest challenge for civilization. Since the pioneer work from Grätzel *et al*. in 1991, dye-sensitized solar cell (DSSC) has been an apparent choice over conventional silicon solar cells owing to their affordable production cost, light fabrication and relatively high solar to current conversion efficiencies.[1-2] DSSCs assembled with ruthenium complexes as sensitizers gave excellent performance with efficiencies of 11%.[3] Although ruthenium dyes featured advantages like broad absorption, suitable energy levels and higher efficiencies, the drawbacks of moderate extinction coefficients, restricted availability, and higher purification cost hampers their practical application. Nature utilizes chlorophyll in plants as antennae to harvest light for solar energy conversion in photosynthesis. The porphyrins regarded as artificial chlorophylls, gained huge attention in recent years due to their strong absorption in visible region, high absorption coefficients, better thermal and photo-stability and appropriate energy levels. Moreover their optical and electrochemical properties can be fine-tuned through varying substituents on four *meso* and eight *beta* positions. A glimpse of better performance of porphyrins was displayed in 2007, when officer *et al*. reported *beta*-substituted zinc porphyrins with 7.1% efficiency.[4] This result was further bettered in 2010, with a *meso*-linked zinc porphyrin with a push-pull framework with 11% solar conversion efficiency.[5] In 2011, Yella *et al*. reported a Zn(II) porphyrin having long alkoxyl chains to wrap the porphyrin core to suppress the aggregation with a D-π-A structure showing remarkable power conversion efficiency of 12.3% when combined with an organic dye in Co(II/III) tris(bipyridyl)-based redox electrolyte under standard AM 1.5G simulated sunlight.[6] Extensive literature survey on porphyrin sensitized solar cells revealed that the design of the sensitizers is restricted to the regular free-base or zinc porphyrins.[7-10] From the above mentioned examples of regular porphyrin sensitizers, it is estimated that the near-infrared (NIR) absorption and panchromatic spectral character might enhance the solar to current conversion efficiency of DSSCs. The bathochromic absorption enhancement is achieved through extension of π conjugation of these regular porphyrins either by substitutions on *meso*- and *beta*-positions or fusion with aromatic chromophores.[9]

Core modification of the porphyrin core by replacing one or more pyrrolic nitrogens in porphyrin ring with heteroatoms like oxygen, sulphur, selenium and tellurium is an alternative and effective approach to adjust the photophysical properties of porphyrins.[11-12] This core alteration induces interesting variations in photophysical properties of porphyrins without affecting the aromaticity of the macrocycle.[13] Based on these improved optical properties, core-modified porphyrins have

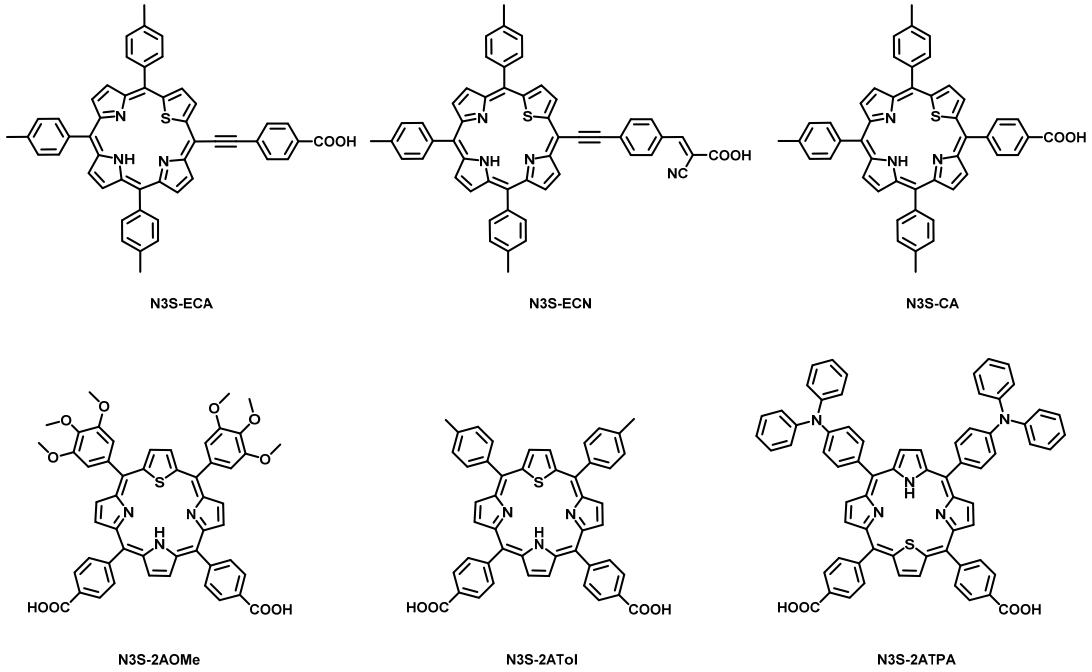

Scheme 1. Chemical structures of A_3B and A_2B_2 thiaporphyrin dyes.

been widely used as complexation agents for metal ions in unusual oxidation states[11] and as photosensitizers in photodynamic therapy.[14-19] A variety of mono-functionalized thiaporphyrins have been reported in the literature,[20-21] but the synthesis of carboxyl functionalized thiaporphyrins are quite rare.[22] Although these thiaporphyrins possess interesting optical properties, surprisingly their use in DSSCs is very uncommon.[23] Following our interest in thiaporphyrins and their metal complexes,[24-25] we have recently shown that these heteroporphyrins can be successfully applied as sensitizers in DSSCs.[26-27] Thiaporphyrin N3S-ECA with an ethynylphenyl linker at a *meso* position and a carboxylic acid as the terminal anchoring group, obtained minute efficiency with iodine/triiodide redox electrolyte.[27] As an attempt to improve the properties of thiaporphyrins-based DSSCs, we explored some possibilities of structural modification on *meso* substituents of thiaporphyrin in order to get higher light harvesting efficiency (LHE) in NIR region.

In this report, we designed and synthesized novel A_3B thiaporphyrins as shown in Scheme 1, with (N3S-ECA) or without (N3S-CA) ethynylphenyl linker along with using either simply carboxylic acid or cyanoacrylic acid (N3S-ECN) as the anchoring group. Also, A_2B_2 thiaporphyrins possessing two carboxylic acid anchors on *cis*-position in conjunction with donors like, 3,4,5-trimethoxy (N3S-2AOMe), tolyl (N3S-2ATol) and triphenylamine (N3S-2ATPA) are prepared for comparison. The effect of one anchor versus two anchors as well as the effect of ethynylphenyl linker and the electron withdrawing cyano group on the photophysical properties of the thiaporphyrins are studied. The systematic study, well supported by optical spectroscopy, CV measurements, DFT calculations, attenuated total reflectance Fourier transform infrared spectroscopy (ATR-FTIR), and photovoltaic measurements revealed the marked significance of ethynylphenyl linker and electron-withdrawing cyano group to the overall photon conversion efficiencies.

Results and discussion

Syntheses

The A_3B thiaporphyrin dyes were synthesized according to the stepwise synthetic protocol depicted in Scheme 2. The synthesis of N3S-ECA was previously reported.[27] N3S-ECN was prepared from N3S-Br (1) and 4-ethynylbenzaldehyde through Sonogashira coupling in the presence of palladium catalyst. Compound (2) was further condensed with cyanoacetic acid following Knoevenagel protocol to obtain N3S-ECN. The presence of acrylic proton in the downfield region at 8.39 ppm in ^{1}H NMR spectrum of N3S-ECN confirmed the formation of cyano derivative. The presence of the cyano group is further confirmed by the presence of CN stretching frequency around 2224 cm^{-1} in the IR spectrum. In order to get N3S-CA, thiophene was treated with *p*-tolualdehyde and methyl-4-formylbenzoate in presence of *n*-BuLi to get unsymmetrical diol (3) as shown in Scheme 2. The mixed condensation of this unsymmetrical diol (3) with *p*-tolualdehyde and pyrrole in the presence of boron trifluoride-diethyl etherate as catalyst, followed by consequent oxidation by 2,3-dichloro-5,6-dicyanobenzoquinone (DDQ) gave monoester compound (4), which was further hydrolysed by aqueous solution of KOH to yield N3S-CA. The A_2B_2 thiaporphyrin dyes were synthesized according to the stepwise synthetic protocol depicted in Scheme 3.

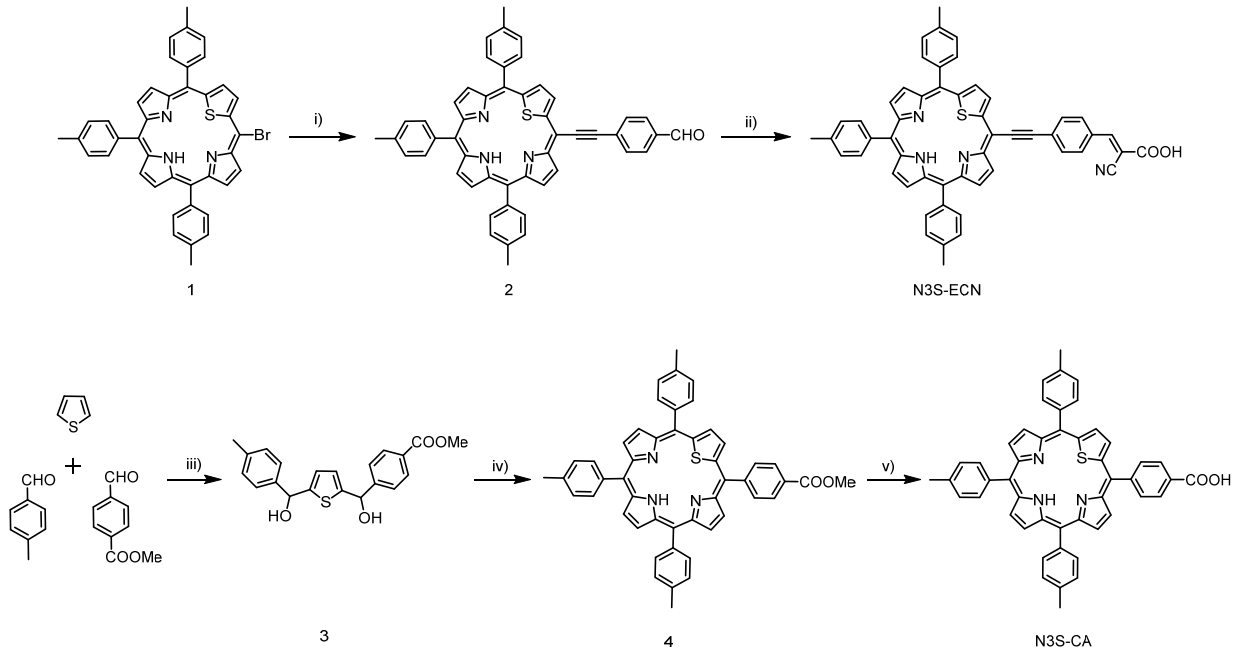

Scheme 2. Synthesis of A_3B thiaporphyrins. Reagents and conditions: i) 4-ethynylbenzaldehyde, $Pd_2(dba)_3$, $AsPh_3$, THF/NEt_3; ii) cyanoacetic acid, piperidine, $CHCl_3$; iii) *n*-BuLi, TMEDA, Hexane/THF; iv) *p*-tolualdehyde, pyrrole, BF_3•OEt_2, DDQ, CH_2Cl_2; v) $KOH_{(aq)}$, THF.

Thiophene was treated with corresponding aldehydes in the presence of *n*-BuLi to get the desired symmetrical thiophene diols. The mixed-condensation of these symmetrical diols with appropriate aldehydes and pyrrole in the presence of boron trifluoride-diethyl etherate as catalyst, followed by subsequent oxidation by DDQ gave diester compounds. The diester compounds were purified by column chromatography and subsequent hydrolysis by $KOH_{(aq)}$ yielded analytically pure thiaporphyrins. The carbonyl stretching peaks around 1680-1700 cm^{-1} in the final carboxylic acid substituted compounds are slightly shifted to lower energy compared with their ester derivatives due to the intermolecular hydrogen bonding.

Absorption and Emission properties

The UV-Visible peak positions of the *Soret* and Q-bands and the molar absorption coefficients (ε) of thiaporphyrins in THF are summarized in Table 1. The UV-Visible spectra of the studied porphyrins as displayed in Figure 1, shows typical free-base porphyrin features including a strong *Soret* band around 430 nm and four Q-bands around 510-700 nm. The absorption wavelengths of these thiaporphyrins depend mainly on the nature of the substituents. The introduction of ethynylphenyl linker at a *meso* carbon significantly shifts the absorption wavelength towards low energy region as shown in N3S-ECA and N3S-ECN compared to N3S-CA. The UV-Visible spectrum of N3S-ECN, having a cyanoacrylic acid terminal as the anchor shows the largest red-shift in the *Soret* band as well as Q-bands, extending the absorption onset beyond 700 nm. The electron donating triphenylamine substituents on *meso* positions in N3S-2ATPA result in the broadening of *Soret* band as compared to N3S-2ATol and N3S-2AOMe. The extinction coefficient of N3S-CA is the highest amongst the thiaporphyrins. Although the ε is not high for N3S-ECN and N3S-2ATPA, the IPCE (incident photon-to-current efficiency) might be compensated by the broadened absorption and increased electron injection resulting in a higher overall conversion efficiency. (*vide infra*)

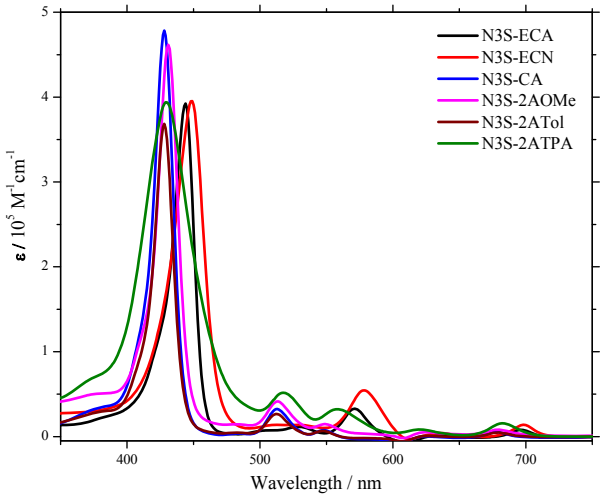

Figure 1. UV-Visible spectra of thiaporphyrin dyes in THF.

The absorption spectra of these thiaporphyrins as thin films were studied to understand their adsorption behaviour on TiO_2.

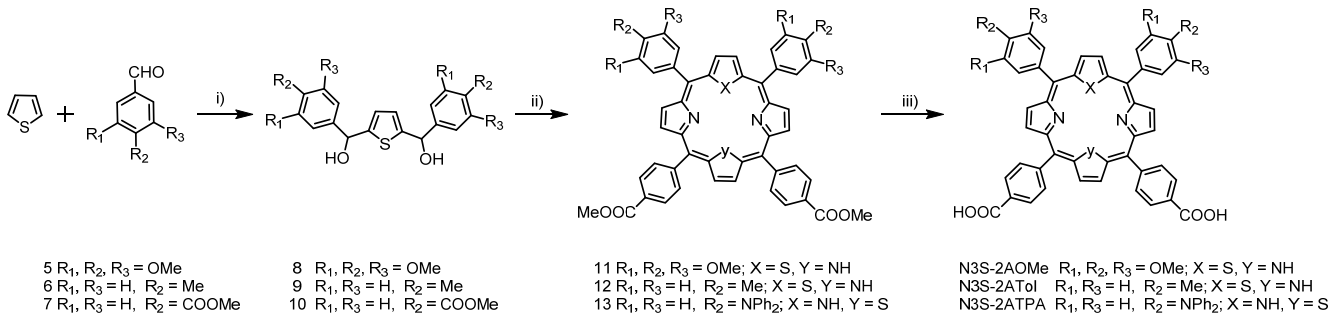

5 R_1, R_2, R_3 = OMe
6 R_1, R_3 = H, R_2 = Me
7 R_1, R_3 = H, R_2 = COOMe

8 R_1, R_2, R_3 = OMe
9 R_1, R_3 = H, R_2 = Me
10 R_1, R_3 = H, R_2 = COOMe

11 R_1, R_2, R_3 = OMe; X = S, Y = NH
12 R_1, R_3 = H, R_2 = Me; X = S, Y = NH
13 R_1, R_3 = H, R_2 = NPh_2; X = NH, Y = S

N3S-2AOMe R_1, R_2, R_3 = OMe; X = S, Y = NH
N3S-2ATol R_1, R_3 = H, R_2 = Me; X = S, Y = NH
N3S-2ATPA R_1, R_3 = H, R_2 = NPh_2; X = NH, Y = S

Scheme 3. Synthesis of A_2B_2 thiaporphyrins. Reagents and conditions: i) *n*-BuLi, TMEDA, hexane/THF; ii) aldehyde, pyrrole, BF_3•OEt_2, DDQ, CH_2Cl_2; iii) $KOH_{(aq)}$, THF.

Table 1. Optical and Electrochemical data of thiaporphyrin dyes

Dye	λ_{abs} [a] [nm] ($\varepsilon/10^3 M^{-1}cm^{-1}$)	λ_{em} [b] [nm]	E_{ox} [c] [V]	$E_{(0,0)}$ [d] [eV]	E_{ox}* [e] [V]
N3S-ECA	444 (393), 530 (13), 571 (34), 634 (3), 697 (9)	702 777	0.96	1.77	− 0.81
N3S-ECN	449 (396), 526 (15), 579 (55), 637 (5), 698(15)	705 779	0.97	1.77	− 0.80
N3S-CA	428 (504), 513 (35), 548 (9), 625 (1), 678 (7)	684 751	0.91	1.82	− 0.91
N3S-2AOMe	431 (438), 513 (39), 549 (14), 625 (5), 679(8)	688 755	0.94	1.81	− 0.87
N3S-2ATol	428 (369), 512 (28), 547 (8), 624 (2), 679 (6)	686 754	0.93	1.82	− 0.89
N3S-2ATPA	429 (394), 518 (52), 558 (32), 621 (8), 682 (16)	693 757	0.90	1.80	− 0.90

[a]Absorption maximum of porphyrins in THF. [b]Emission maximum measured in THF by exciting at Soret band. [c]Oxidation potentials approximated from E_{ox}* and $E_{(0,0)}$. [d]$E_{(0,0)}$ values were estimated from the intersection of the absorption and emission spectra. [e]First reduction potentials vs. NHE determined for A_3B by cyclic voltammetry and for A_2B_2 by square wave voltammetry in THF and referenced to a ferrocene redox couple.

To obtain the absorption spectra on TiO_2 films, the films with thickness of approximately 3 μm were dipped in 0.1 mM THF solution of thiaporphyrins for 8 h at room temperature. The adsorption spectra were recorded by reflectance measurements using an integrated sphere and the results are displayed in Figure 2. The absorption spectra of dyes adsorbed on TiO_2 show significant broadening and slightly redshifts compared to its absorption spectrum in THF with threshold of absorption around 750 nm.[28-29] Particularly, the UV-Visible spectrum of N3S-ECN/TiO_2 and N3S-2ATPA/TiO_2 shows obvious broadening and bathochromic shifts. This broadening in the UV-Vis spectra after adsorption on TiO_2 films suggests that higher charge collection is possible in Q-band region which will ultimately help to attain higher efficiency when applied in DSSC. The steady-state fluorescence spectra of all the porphyrins were measured in THF by excitation at the *Soret* band and displayed in Figure 3.

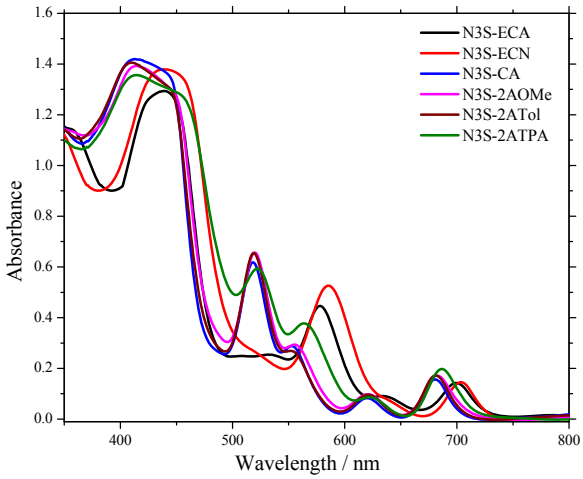

Figure 2. UV-Visible spectra of dyes/TiO_2

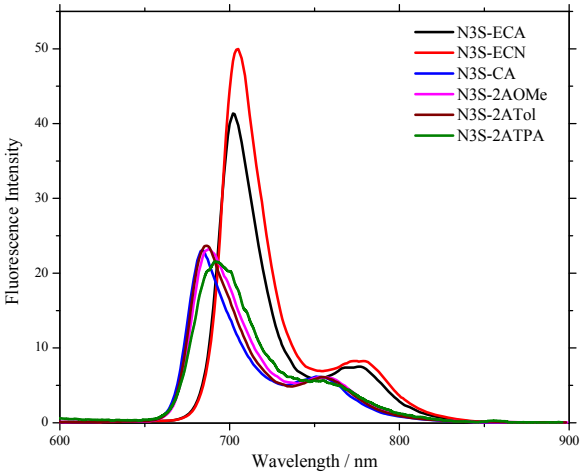

Figure 3. Fluorescence spectra of thiaporphyrin dyes in THF

It exhibited a trend similar to the absorption spectra, with a significant redshift upon addition of ethynylphenyl linker. Not only the redshift but also higher fluorescence intensity of N3S-ECA and N3S-ECN suggests that the conjugation through ethynylphenyl linker is more effective than direct phenyl substitution which might result in better electron communication between porphyrin core and the anchoring group.

Electrochemical studies

For the efficient electron injection into TiO_2 and faster regeneration of the oxidized dyes, appropriate toning of highest occupied molecular orbitals (HOMO) with iodide/triiodide couple and the lowest unoccupied molecular orbitals (LUMO) with TiO_2 conduction band is necessary. The cyclic voltammetry measurements of all the thiaporphyrins were carried out in degassed THF containing 0.1 M $[Bu_4N]PF_6$ as the supporting electrolyte to obtain the first reduction potentials as depicted in Figure 4. The first reduction couples of N3S-ECA, N3S-ECN and N3S-CA show quasi-reversible redox processes under a scan rate of 50 mV/s while irreversible processes of the first reduction couple were observed for thiaporphyrins with dual carboxyphenyl substituents, N3S-2AOMe, N3S-2ATol and N3S-2ATPA. The reduction potentials for thiaporphyrins with a *meso* ethynylphenyl substituent are less negative than the rest thiaporphyrins. The zero-zero excitation energies, $E_{(0,0)}$ were calculated from the intersection of the normalized absorption and emission spectra at the Q (0,0) band and were found to be 1.77, 1.77, 1.82, 1.81, 1.82 and 1.80 eV for N3S-ECA, N3S-ECN, N3S-CA, N3S-2AOMe, N3S-2Atol and N3S-2ATPA porphyrins, respectively. The oxidation potentials were estimated from the first reduction potentials and the zero-zero excitation energies and are listed in Table 1.

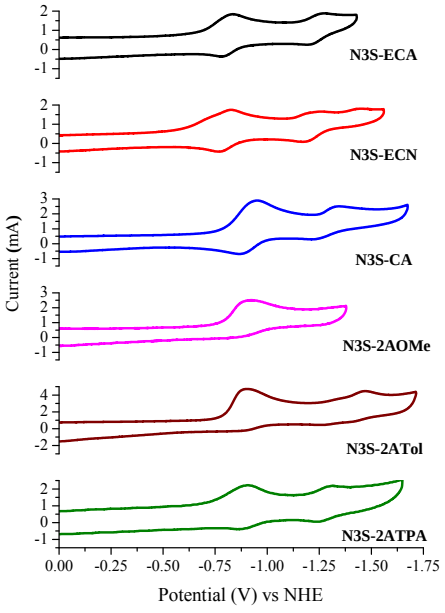

Figure 4. Cyclic Voltammograms of thiaporphyrin dyes in THF.

The systematic energy level diagram for the studied thiaporphyrins is displayed in the Figure 5. As evident from the energy level diagram, the ethynylphenyl substitution results in the smaller HOMO and LUMO band gaps and consequently red shifting the absorption for A_3B thiaporphyrins compared to those without an ethynylphenyl linkage. For A_2B_2 thiaporphyrins, the $E_{(0,0)}$ decreases with increasing electron donating ability of the thiaporphyrins. The LUMO of the thiaporphyrins are more negative than the TiO_2 conduction band (> 0.3 V) and thus ensure the adequate driving force for the electron injection from dye to the TiO_2 conduction band. The HOMO of all the porphyrins are more positive (> 0.5 V) than the redox electrolyte which confirms the efficient dye regeneration.

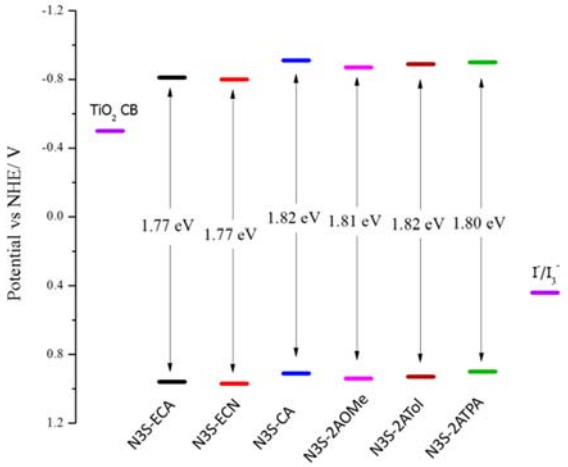

Figure 5. Energy level diagram for thiaporphyrin dyes under study.

DFT Calculation results

The ground state geometries of studied thiaporphyrins were optimized in the gas phase by DFT calculations using the hybrid B3LYP functional and the 6-31G basis set. As presented in Figure 6, result from the quantum chemical calculations show planar macrocycles for the studied thiaporphyrins. The planar ring ensures the effective electron coupling between the porphyrin ring and the anchoring group. The HOMO-LUMO energy gaps for all the thiaporphyrins are consistent with the absorption energy obtained from UV-Vis spectra. In N3S-ECA and N3S-ECN, the majority of the π electron density is localized on the porphyrin ring however a small portion is also extended over the anchoring group in HOMO. In the LUMO of N3S-ECA, the electron density is distributed equally on the porphyrin ring, the ethynylphenyl linker and carboxylic acid anchor. In the LUMO of N3S-ECN, more π electron density is localized on the ethynylphenyl linker and anchoring cyano acrylic acid group than on the porphyrin core, which highlights the electron withdrawing effect of the cyano group. For N3S-CA, N3S-2AOME, N3S-2Atol and N3S-2ATPA, the majority of the electron density in HOMO as well as LUMO is located on the porphyrin ring suggesting that the charge transfer in

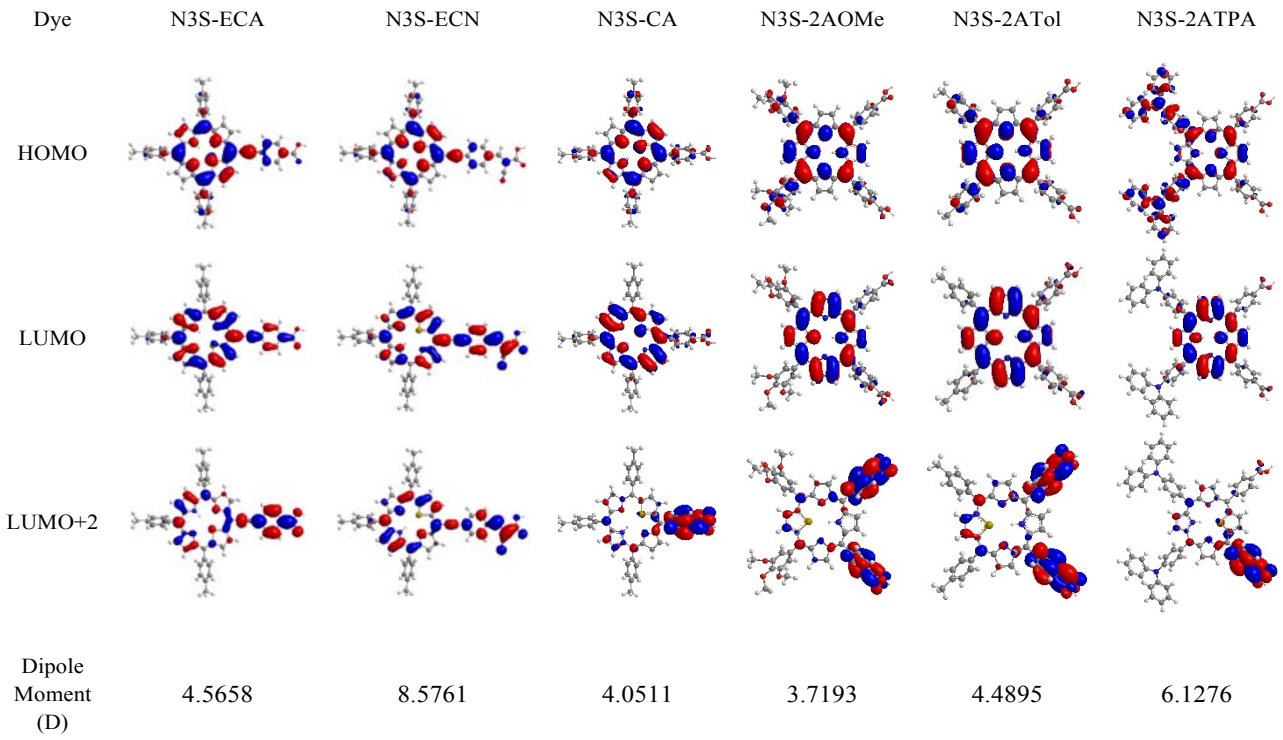

Figure 6. The molecular orbital diagrams for thiaporphyrin dyes.

these porphyrins might be less efficient than the *meso* ethynylphenyl substituted derivatives. Thus based on the theoretical calculations, it is evidenced that the ethynylphenyl linker is highly beneficial for an efficient electron transfer from the porphyrin core to the electron withdrawing anchoring group. This effective electron distribution, especially in the case of N3S-ECN facilitates efficient charge transfer from the excited state of the porphyrins to the TiO_2 conduction band. Interestingly in the LUMO+2, the electron density is extensively located on the carboxylic acid acceptor suggesting that the electron injection from higher excited states involving LUMO+2 might be possible. The dipole moments for thiaporphyrins under study were estimated from theoretical calculations and displayed in Figure 6. The dipole moments decrease in the order N3S-ECN > N3S-2ATPA > N3S-ECA > N3S-2ATol > N3S-CA > N3S-2AOMe. The trend of dipole moments is consistent with the overall conversion efficiency for these thiaporphyrins except for N3S-ECA. N3S-ECA might have higher dipole moment (4.56 D) than N3S-CA due the presence of ethynyl linker. The highest dipole moment of 8.57 D is observed for N3S-ECN, highlighting the effectiveness of electron withdrawing cyano acrylic anchoring group. The higher polarizability is advantageous to expedite intramolecular photoinduced electron transfer.

ATR-FTIR studies

ATR-FTIR spectroscopy measurements have been utilized as one of the imperative tools for probing the number and mode of carboxylate groups anchored onto TiO_2.[30-33] The ATR-FTIR spectra of neat thiaporphyrins contrasted with spectra of thiaporphyrins adsorbed on TiO_2. Comparative spectra of representative samples are shown in Figure 7. The spectra of neat N3S-CA and N3S-2ATol show strong ν(C=O) stretches at 1687 and 1686 cm^{-1}, respectively, whereas ν_{sym} (COO^-) and ν_{asym} (COO^-) stretches are likely to be observed at about 1400 and 1600 cm^{-1}, respectively. In the comparative spectra of N3S-CA/TiO_2 and N3S-2ATol/TiO_2, the ν(C=O) stretches completely disappeared, accompanied by a noticeable rise in the stretching peaks of ν_{sym} (COO^-) and ν_{asym} (COO^-) at about 1400 and 1600 cm^{-1}, respectively. The observation noted above indicates that for N3S-CA bonding on to TiO_2 is achieved through one carboxyl group while in N3S-2ATol, both *p*-carboxyphenyl groups at the *cis* positions are used for bonding onto TiO_2. Similar observations are found for the remaining thiaporphyrins, that is, N3S-ECA, N3S-ECN, N3S-2AOMe and N3S-2ATPA (ESI, Figure S1). Based on the above analyses, the single-anchoring mode for A_3B thiaporphyrins and dual-anchoring mode for A_2B_2 thiaporphyrins is proposed for the attachment of the porphyrins onto TiO_2.

Dye loading results

To better comprehend the adsorption behavior and measure the amount of adsorbed dye, we calculated the dye densities adsorbed on TiO_2 surface. The porphyrin densities (Γ) were determined by measuring the absorbance of porphyrins desorbed from the sensitized TiO_2 films after being immersed in 0.1 M KOH solution in THF.

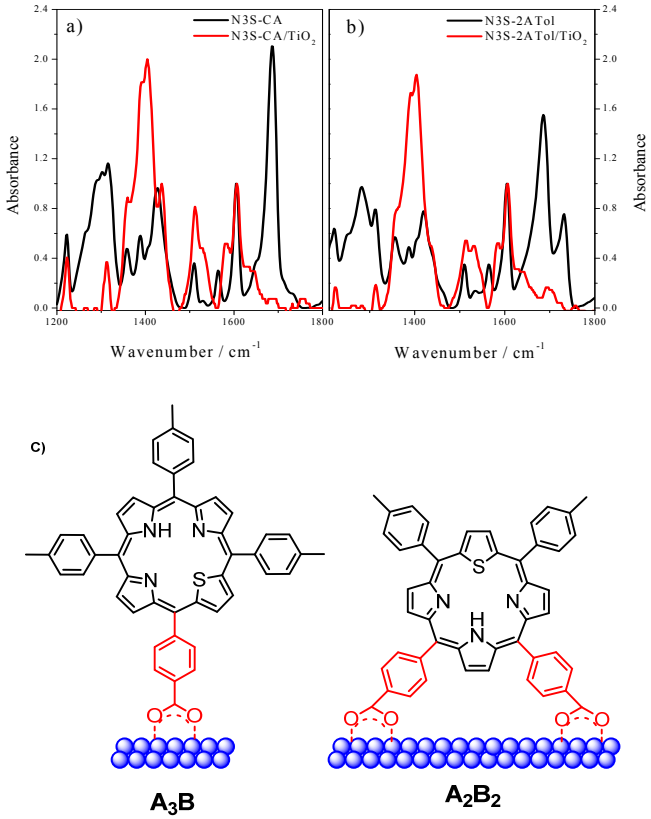

Figure 7. ATR-FTIR spectra of a) N3S-CA and N3S-CA/TiO_2 and b) N3S-2ATol and N3S-2ATol/TiO_2; the ATR-FTIR spectra of the thiaporphyrins on TiO_2 are normalized for comparison. c) Possible modes of attachment of thiaporphyrins onto TiO_2. For demonstration purpose only, the relative sizes of the molecules and nanoparticles are not correlated in real dimensions.

The saturated Γ values of A_3B thiaporphyrins under study were found as 141 ± 13, 144 ± 11 and 100 ± 8 nmol cm^{-2} for N3S-ECA, N3S-ECN and N3S-CA. Due to the ethynylphenyl substitution the thiaporphyrins N3S-ECA and N3S-ECN became planar compared to N3S-CA, giving dense packing on the TiO_2 surface resulting in higher dye loadings. The Γ values for A_2B_2 thiaporphyrins N3S-2AOMe, N3S-2ATol and N3S-2ATPA are found as 85 ± 5, 116 ± 3 and 54 ± 8 nmol cm^{-2}, respectively. The dye loading values for A_2B_2 thiaporphyrins are inversely proportional to the steric bulkiness of the substituents. More bulky the substituent, less is the dye loading. Comprehensively, the dye loading amounts for A_2B_2 thiaporphyrins are lower than that of the A_3B thiaporphyrins. This can be explained with the help of dye attachment mode on the TiO_2 surface. As seen from the ATR-FTIR studies, A_2B_2 thiaporphyrins binds through dual anchoring mode while A_3B thiaporphyrins binds through the single anchoring carboxylic group to the TiO_2 surface. Thus A_2B_2 thiaporphyrins requires more space on the TiO_2 surface compared to the A_3B thiaporphyrins thus giving less dye loadings. It is obvious that higher dye loading is observed for N3S-ECA and N3S-ECN as compared to other thiaporphyrins. The trends in the dye loading amounts mentioned above is not consistent with the efficiency with an exception of N3S-ECN, which has both, higher dye loading as well as higher efficiency. Regardless of low dye loading, N3S-2ATPA gave superior performance with higher current density.

Photovoltaic studies

Devices assembled with thiaporphyrin sensitizers using liquid electrolytes were tested under standard AM 1.5 illumination conditions. The photovoltaic parameters for the thiaporphyrins under study are summarized in Table 2 and the current-voltage characteristics of the devices are shown in Figure 8a.

Table 2: Photovoltaic parameters of thiaporphyrin dyes

Dye	*J*sc (mA cm^{-2})	*V*oc (V)	*ff* (%)	*η* (%)
N3S-ECA	0.89	0.41	0.55	0.20
N3S-ECN	5.12	0.49	0.67	1.69
N3S-CA	1.29	0.48	0.64	0.40
N3S-2AOMe	0.67	0.45	0.57	0.17
N3S-2ATol	1.52	0.47	0.65	0.46
N3S-2ATPA	2.84	0.48	0.63	0.86

As evident from the I-V curve, the N3S-ECN give the best performance with the overall photon-to-current conversion efficiency of 1.69%, supported by short-circuit current (*J*sc) of 5.12 mA cm^{-2}, open-circuit voltage (*V*oc) of 0.49 V and fill factor (ff) of 0.67. It is well reinforced by DFT calculations and photophysical studies that the electron-withdrawing cyano acrylic acid terminal group enhances the charge transfer from porphyrin ring towards the anchoring group. Also due to the electron withdrawing cyano group, the LUMO level of N3S-ECN is closer to the TiO_2 conduction band compared to other thiaporphyrins, which may facilitate the electron injection. The higher electron injection from the dye to the TiO_2 conduction band is well reflected by the much higher short-circuit current for N3S-ECN. Although the *V*oc values are all alike, other A_3B and A_2B_2 thiaporphyrins have low *J*sc values and therefore, inferior power conversion efficiencies. Noticeably, N3S-ECA only obtained short-circuit current of 0.89 mA cm^{-2}, open-circuit voltage of 0.41 V and fill factor 0.55 corresponding to photon-to-current conversion efficiency of 0.20%. It suggests that carboxylic acid alone is not sufficient to pull more electrons from the porphyrin core towards the anchor which results in the lower performance of N3S-ECA. Interestingly N3S-CA, without a *meso* ethynylphenyl linker, achieved higher efficiency of 0.40% with short-circuit current of 1.29 mA cm^{-2}, open-circuit voltage of 0.48 V and fill factor of 0.64. The A_2B_2 thiaporphyrin, N3S-2ATol with two anchoring carboxylic groups obtained the overall photon-to-current conversion efficiency of 0.46% with photocurrent density of 1.52 mA cm^{-2},

open-circuit voltage of 0.47 V and fill factor of 0.65, which is slightly higher than single arm anchoring dye, N3S-CA. Among the thiaporphyrins, N3S-2AOMe gave the least conversion efficiency of 0.17% with short-circuit current of 0.67 mA cm^{-2}, open-circuit voltage of 0.45 V and fill factor of 0.57. This might be due to lower dye loadings as compared to other thiaporphyrins. Thiaporphyrin substituted with triphenylamine donor, N3S-2ATPA gave the highest efficiency among A_2B_2 thiaporphyrins. It obtained conversion efficiency of 0.86%, with *J*sc = 2.84 mA cm^{-2}, *V*oc = of 0.48 V and fill factor of 0.63. The trend of *J*sc in this series can be understood from the variation of the IPCE spectra as displayed in Figure 8b and are in good agreement with the corresponding absorption spectra of the dyes on TiO_2 which display intense absorption bands in the *Soret* region.

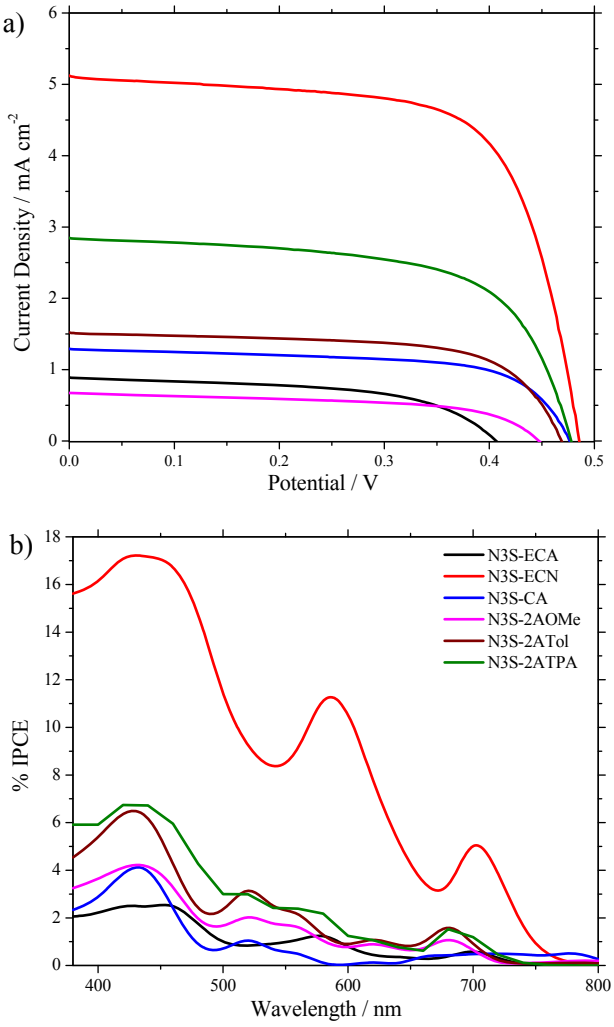

Figure 8. (a) I-V curves and (b) IPCE spectra for A_3B and A_2B_2 thiaporphyrin dyes.

The *J-V* curves under standard AM 1.5 G illumination are in qualitative agreement with the photo-action spectra of these thiaporphyrins. For N3S-ECN the IPCE maximum is around 17% in the *Soret* region, while around 12% in the 550-600 nm region and 6% in the 700 nm region. This indicates that N3S-ECN shows panchromatic absorption behaviour covering whole visible region. This increased photon collection explicates the higher short-circuit current for this compound. In case of N3S-ECA and N3S-CA, there is insignificant IPCE in Q-band region which is one of the reasons for their inferior performance compared to N3S-ECN. Even though the IPCE values are higher for N3S-2AOMe than N3S-ECA and N3S-CA, the lower dye density triggered by bulky methoxy groups might be the reason for its low efficiency.

Electrochemical Impedance Spectroscopy results

To further study the correlation between the charge transfer processes and photovoltaic properties in the DSSC devices with different thiaporphyrin sensitizers, electrochemical impedance spectroscopy (EIS) was measured under illumination with an open-circuit voltage with a frequency range of 1 Hz to 1 kHz. Figure 9 shows the EIS Nyquist plots (i.e. the minus imaginary part of the impedance Z" vs. the real part of the impedance Z' when sweeping the frequency) for DSSCs based on thiaporphyrins. One semicircle was observed for all the thiaporphyrins in the Nyquist plots. This semicircle corresponds to the charge transfer processes at the TiO_2–dye–electrolyte interface *i*.e. electron transport resistance.[34] A smaller radius of the semicircle in the Nyquist plot corresponds to the lower electron transport resistance, in other words higher electron transfer. The radius of the semicircle in the Nyquist plot decreases in the order N3S-2AOMe > N3S-2ATol > N3S-CA >N3S-ECA > N3S-2ATPA > N3S-ECN. This trend is roughly consistent with the DSSC performance of the thiaporphyrin sensitizers. The DSSC based on N3S-ECN exhibited smaller interfacial charge transfer resistance at the dye-TiO_2-electrolyte interface compared to other dyes indicating improved charge generation and transport, which is well reflected in its higher photocurrent density.

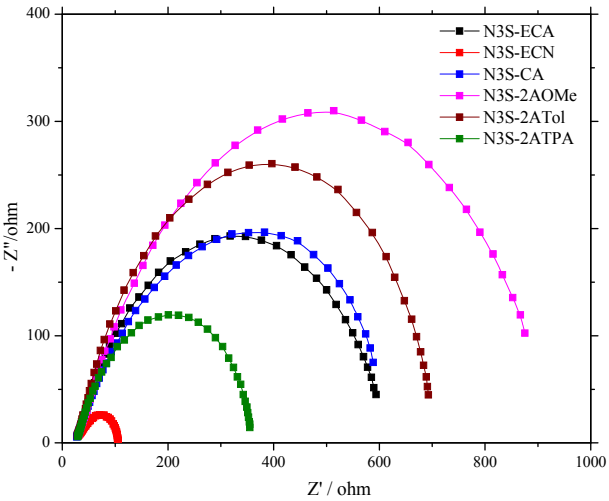

Figure 9. Impedance spectra (Nyquist plots) of DSSCs based on thiaporphyrins measured under illumination.

Conclusion

In summary, we have prepared novel mono- and di- carboxylate functionalized A_3B and A_2B_2 thiaporphyrins. With the support of the photophysical and photovoltaic data, it is revealed that these thiaporphyrins, after systematic structural modification can be applied in dye-sensitized solar cells. The UV-Visible spectra of these thiaporphyrins displayed that ethynyl phenyl linker effectively enhances the absorption wavelengths towards near infra-red region. Density functional theory calculations show that, higher π electron density is localized on the cyano acrylic acid anchor in lower unoccupied molecular orbital of N3S-ECN compared to other thiaporphyrins; consequently, more electrons are available for injection from the dye into the conduction band of TiO_2. As seen from the electrochemical properties and energy level diagram, the energy levels of the thiaporphyrins are suitable for application as a sensitizer in dye-sensitized solar cells. The best conversion efficiency of 1.69% with high photocurrent density of 5.12 mA cm^{-2} is obtained for N3S-ECN owing to their superior photophysical properties. To the best of our knowledge this is the highest efficiency for thiaporphyrin-based dye-sensitized solar cells. These results suggests that the thiaporphyrins, core-modified derivatives of porphyrins, can serve as effective sensitizers for future dye-sensitized solar cell applications.

Experimental

General Methods

All chemicals were obtained from commercial sources and used as received without further purification. All the reactions were carried out under nitrogen atmosphere. Solvents used in reactions were dried by PureSolv MD 5 system **(**Innovative Technology, Inc). Flash chromatography was carried out by using silica gel (40-63 μm, Merck). Analytical TLC was performed on Merck silica gel plates. ^{1}H NMR spectra were recorded on a Bruker 400 MHz spectrometer and performed in $CDCl_3$ (δ = 7.26 ppm), THF-D_8 (δ = 1.73, 3.58 ppm) or DMSO-D_6 (δ = 2.50 ppm) solutions. ^{13}C NMR spectra were performed in $CDCl_3$ (δ = 7.26 ppm) DMSO-D_6 (δ = 40.0 ppm) solutions. Chemical shifts are reported in ppm. Coupling constants *J* are reported in Hz. The signals are described as s: singlet; d: doublet; dd: doublet of doublet. The ESI ion trap mass spectra were measured by a Finnigan MAT LCQ mass spectrometer. The HR-FAB spectra were conducted on a JMS-700 double focusing mass spectrometer. Transmittance and reflection UV–visible absorption spectra of the thiaporphyrins in THF and adsorbed on TiO_2 electrodes, respectively, were recorded on a JASCO V-670 UV–Vis/NIR spectrophotometer. Steady-state fluorescence spectra were acquired by using a Varian Cary Eclipse fluorescence spectrophotometer. The cyclic voltammetry measurements of all thiaporphyrins were carried out on CHI 621B electrochemical analyser (CH Instruments, Austin, TX, USA) in degassed THF containing 0.1 M tetrabutylammonium hexafluorophosphate (Bu_4NPF_6) as the supporting electrolyte. The cell assembly consists of a glossy carbon as the working electrode, a silver wire as the pseudo-reference electrode, and a platinum wire as the auxiliary electrode. The scan rate for all measurements was fixed at 50 mV/sec. A ferrocene$^{+1/0}$ redox couple was used as the internal standard and the potential values obtained in reference to the silver electrode were converted to the vacuum scale. DFT calculations were performed using Gaussian 09 package.[35] The molecular orbitals were visualized by the chem-office software.

Syntheses

The precursors 4-ethynylbenzaldehyde, thiophene diols,[36] 5-bromo-10,15,20-tris(p-tolyl)-21-thiaporphyrin (1)[37-38] and N3S-ECA[27] were prepared by following the reported procedures.

5-(4-Ethynylbenzaldehyde)-10,15,20-tris(*p*-tolyl)-21-thiaporphyrin (2): Bromothiaporphyrin, N3S-Br (1) (100 mg, 0.15 mmol), $Pd_2(dba)_3$ (55 mg, 0.06 mmol), $AsPh_3$ (113 mg, 0.37 mmol) and 4-ethynylbenzaldehyde (25 mg, 0.18 mmol) were added to a 100 ml round bottom flask and the flask is attached to high vacuum for 30 min. Then N_2 was flushed for 15 min and anhydrous THF (40 ml) and triethylamine (10 ml) were added. The reaction mixture was stirred under N_2 at room temperature for 12 h. After completion of the reaction as confirmed by TLC, the solvent was removed under pressure and the crude product was purified by column chromatography using Hexanes/DCM (2/1) as eluent to afford the desired porphyrin (2) as a purple solid (76 mg, 70%). ^{1}H NMR (400 MHz, $CDCl_3$) δ: −2.18 (s, 1H, NH) 2.70 (s, 3H, CH_3), 2.72 (s, 6H, CH_3), 7.53-7.66 (m, 6H, *m*-tolyl), 8.03-8.09 (m, 6H, *o*-tolyl), 8.16 (m, 4H, Ar), 8.54 (d, 1H, J = 4.48 Hz; β-pyrrole), 8.61 (d, 1H, J = 4.52 Hz; β-pyrrole), 8.66 (d, 1H, J = 4.48 Hz; β-pyrrole), 8.86 (s, 2H, β-pyrrole), 9.34 (d, 1H, J = 4.48 Hz; β-pyrrole), 9.83 (d, 1H, J = 5.16 Hz; β-thiophene), 10.14 (s, 1H, CHO), 10.32 (d, 1H, J = 5.16 Hz; β-thiophene) ppm; ^{13}C NMR (100 MHz, $CDCl_3$) δ: 21.53, 94.56, 97.69, 108.52, 124.99, 126.02, 127.39, 127.48, 128.46, 128.75, 129.38, 129.92, 130.07, 131.64, 132.25, 132.98, 133.08, 134.17, 134.25, 134.33, 135.20, 135.67, 135.82, 136.13, 137.67, 137.77, 137.90, 139.00, 139.30, 139.77, 146.23, 150.34, 154.41, 154.49, 157.96, 158.87, 191.41 ppm; HRMS-ESI: m/z calcd for $C_{50}H_{36}N_3OS$: 726.2579, found 726.2582 $[M+H]^+$.

N3S-ECN: To a mixture of thiaporphyrin-CHO (2) (100 mg, 0.13 mmol) in $CHCl_3$ (25 ml) and piperidine (128 μl, 1.3 mmol) was added cyanoacetic acid (46 mg, 0.52 mmol) and the reaction mixture is refluxed for 12 h under N_2. To this mixture 50 ml $CHCl_3$ and 100 ml water were added and transferred to a separation funnel. The pH value of this mixture is adjusted to approximately 2 with 2 M H_3PO_4. The $CHCl_3$ was removed by azeotropic distillation using acetonitrile in vacuo. Precipitation from the resulting acetonitrile solution (50 ml) using H_2O gave N3S-ECN purple solid (90 mg, 87%). ^{1}H NMR (400 MHz, THF-*d*8) δ: −2.08 (s, 1H, NH) 2.68 (s, 3H, CH_3), 2.70 (s, 6H, CH_3), 7.59 (m, 4H, *m*-tolyl), 7.69 (d, 2H, J = 7.8 Hz; *m*-tolyl), 8.06 (m, 4H, *o*-tolyl), 8.15 (d, 2H, J = 7.84 Hz; *o*-tolyl), 8.25 (d, 2H, J = 8.36 Hz; Ar), 8.30 (d, 2H, J = 8.40 Hz; Ph), 8.39 (s, 1H, acryl), 8.48 (d, 1H, J = 4.56 Hz; β-pyrrole), 8.56 (d, 1H, J =

4.56 Hz; β-pyrrole), 8.62 (d, 1H, J = 4.48 Hz; β-pyrrole), 8.87 (s, 2H, β-pyrrole), 9.39 (d, 1H, J = 4.44 Hz; β-pyrrole), 9.83 (d, 1H, J = 5.20 Hz; β-thiophene), 10.38 (d, 1H, J = 5.16 Hz; β-thiophene) ppm; ^{13}C NMR (100 MHz, DMSO-*d*6) δ: 21.01, 45.39, 91.88, 98.87, 108.54, 114.12, 119.00, 124.58, 124.65, 125.44, 127.48, 127.55, 128.60, 129.06, 129.57, 129.84, 131.92, 132.25, 132.49, 133.04, 133.85, 133.93, 135.29, 135.75, 135.86, 136.61, 137.56, 137.71, 138.01, 138.15, 138.38, 138.78, 145.23, 146.66, 149.04, 153.49, 153.61, 157.03, 157.85, 162.88 ppm; IR (Neat): 3327, 2923, 2860, 2224, 2184, 1697, 1576, 1537, 1422, 1283, 1179, 941, 796, 704; UV-Vis (THF) λ_{max}/nm (ε/10^3 M^{-1} cm^{-1}) = 449 (396), 526 (15), 579 (55), 637 (5), 698 (15); HRMS-ESI: m/z calcd for $C_{53}H_{37}N_4O_2S$: 793.2637, found 793.2635 $[M+H]^+$.

Mixed diol (3): Anhydrous hexane (60 ml) was added to a 500 ml three-necked round-bottomed flask equipped with rubber septum, gas inlet and gas outlet tube. A positive pressure of N_2 was maintained and after purging N_2 gas for 5 min, TMEDA (11.5 ml, 75 mmol) and *n*-BuLi (62 ml of 1.6 M solution in hexane) were added sequentially to the stirring solution at room temperature. Thiophene (2 ml, 25 mmol) was then added and the solution was refluxed for 1 h. As the reaction progressed, a white turbid solution formed indicating the formation of the 2,5-dilithiated salt of thiophene. The reaction mixture was cooled with ice bath and an ice-cold solution of *p*-tolualdehyde (2.95 ml, 25 mmol) and methyl-4-formylbenzoate (4.1 g, 25 mmol) in dry THF (60 ml) was then cannulated to the stirring solution. The resulting reaction mixture was stirred at 0 °C for 15 min and then brought up to room temperature. The reaction was quenched by adding cold saturated NH_4Cl solution (50 ml). The organic layer was washed with brine and dried over anhydrous $MgSO_4$. The solvent was removed on a rotary evaporator under reduced pressure to afford the crude compound. The crude product was further purified by silica gel column chromatography using EA/Hexanes (3:7) as eluent to collect desired diol (3) as yellow solid (1.76 g, 19%). ^{1}H NMR (400 MHz, $CDCl_3$) δ: 2.34 (s, 3H, CH_3), 2.46 (d, 1H, *J* = 3.88 Hz; OH), 2.61 (d, 1H, *J* = 3.76 Hz; OH), 3.90 (s, 3H, OMe), 5.91 (s, 1H, *meso*), 5.99 (d, 1H, *meso*), 6.69 (m, 2H, *m*-tolyl), 7.15 (d, 2H, *J* = 8.00 Hz; Ph), 7.29 (m, 2H, *o*-tolyl), 7.49 (d, 2H, *J* = 2.67 Hz; *β*-thiophene), 8.00 (d, 2H, *J* = 8.16 Hz; Ph) ppm. ^{13}C NMR (100 MHz, $CDCl_3$) δ: 21.13, 52.11, 71.94, 72.41, 124.29, 124.78, 126.13, 129.22, 129.81, 137.85, 139.88, 147.01, 147.10, 147.67, 148.86, 148.95, 166.85 ppm.

N3S-CE (4): In a 500 ml one-necked round-bottomed flask fitted with a N_2 gas bubbler, a solution of the mixed thiophene diol (9) (737 mg, 2 mmol), pyrrole (411 µl, 6 mmol) and *p*-tolaldehyde (471 µl, 4 mmol) in DCM (400 ml) was taken. Resulting reaction mixture was purged with N_2 for 15 min and then a catalytic amount of BF_3•OEt_2 (25 µl, 0.2 mmol) was added at room temperature. After stirring for 1 h, DDQ (908 mg, 4 mmol) was added and the reaction mixture was stirred at room temperature in air for 1 h. The solvent was removed on a rotary evaporator. The crude product was purified by silica gel column chromatography using Hexanes/DCM (1:1) as eluent to afford the desired porphyrin (4) as purple solid. (290 mg, 20%). ^{1}H NMR (400 MHz, $CDCl_3$) δ: −2.65 (s, 1H, NH), 2.71 (s, 9H, CH_3), 4.12 (s, 3H, OMe), 7.56 (d, 4H, *J* = 7.80 Hz; *m*-tolyl), 7.63 (d, 2H, *J* = 7.80 Hz; *m*-tolyl), 8.09 (m, 4H, *o*-tolyl), 8.15 (d, 2H, *J* = 7.88 Hz; *o*-tolyl), 8.35 (d, 2H, *J* = 8.12 Hz; Ph), 8.51 (d, 2H, *J* = 8.24 Hz; Ph), 8.64 (m, 3H, *β*-pyrrole), 8.71 (d, 1H, *J* = 4.60 H, *β*-pyrrole), 8.97 (d, 2H, *J* = 1.72 Hz, *β*-pyrrole), 9.68 (d, 1H, *J* = 5.28 Hz, *β*-thiophene), 9.79 (d, 1H, *J* = 5.32 Hz, *β*-thiophene) ppm. ^{13}C NMR (100 MHz, $CDCl_3$) δ: 21.50, 52.34, 124.11, 124.38, 127.35, 128.32, 128.69, 128.91, 129.03, 129.38, 129.54, 131.86, 132.51, 133.08, 133.55, 134.17, 134.36, 134. 67, 135.58, 135.81, 137.61, 137.99, 139.11, 139.25, 139.46, 145.92, 146.75, 146.92, 154.54, 156.65, 157.62, 167.34 ppm. HRMS-ESI: *m/z* calcd for $C_{49}H_{38}N_3O_2S$: 732.2685, found 732.2684 $[M+H]^+$.

N3S-CA*:* Thiaporphyrin ester (4) (200 mg, 0.27 mmol) was dissolved in 50 mL THF. To this mixture, 20 equivalent of KOH mixed in 10 ml water was added and the reaction mixture was refluxed for 12 h. After cooling, the organic solvent was removed under pressure. 50 mL water was added to the reaction mixture and the solution was treated slowly with 1 N HCl. The precipitation formed were filtered off and washed with distilled water. The residue remained is dissolved in methanol and dried in vacuum to yield the desired porphyrin as purple solid (175 mg, 90%). ^{1}H NMR (400 MHz, DMSO-*d*6) δ: −2.82 (s, 1H, NH), 2.64 (s, 9H, CH_3), 7.62 (m, 6H, *m*-tolyl), 8.08 (m, 6H, *o*-tolyl), 8.34 (d, 2H, *J* = 8.12 Hz; Ph), 8.42 (d, 2H, *J* = 8.16 Hz; Ph), 8.53 (m, 2H, *β*-pyrrole), 8.62 (m, 2H, *β*-pyrrole), 8.97 (d, 2H, *J* = 1.56 Hz, *β*-pyrrole), 9.74 (d, 1H, *J* = 5.28 Hz, *β*-thiophene), 9.78 (d, 1H, *J* = 5.20 Hz, *β*-thiophene), 13.29 (bs, 1H, COOH) ppm. ^{13}C NMR (100 MHz, DMSO-*d*6) δ: 21.04, 124.11, 124.88, 127.53, 128.01, 128.57, 128.71, 129.35, 129.68, 130.41, 131.62, 132.97, 133.22, 133.87, 134.00, 134.42, 135.08, 135.81, 137.08, 137.52, 138.25, 138.40, 138.55, 139.16, 144.43, 145.98, 146.06, 153.75, 156.08, 156.80, 167.41 ppm; IR (neat): 3327, 2917, 2866, 1687, 1608, 1427, 1316, 1222, 1183, 968, 799, 717; UV-Vis (THF) λ_{max}/nm (ε/10^3 $M^{-1}cm^{-1}$) = 428 (504), 513 (35), 548 (9), 625 (5), 679 (8); HRMS-ESI: *m/z* calcd for $C_{48}H_{36}N_3O_2S$: 718.2528, found 718.2534 $[M+H]^+$.

2,5-Bis(3,4,5-trimethoxyphenylmethanol)thiophene (8): Anhydrous hexane (40 ml) was added to a 250 ml three-necked round bottomed flask equipped with rubber septum, gas inlet and gas outlet tube. A positive pressure of N_2 was maintained and after purging N_2 gas for 5 min, TMEDA (4.7 ml, 31.25 mmol) and *n*-BuLi (13 ml of 2.5 M solution in hexane) were added sequentially to the stirring solution at room temperature. Thiophene (1 ml, 12.5 mmol) was then added and the solution was refluxed for 1 h. As the reaction progressed, a white turbid solution formed indicating the formation of the 2,5-dilithiated salt of thiophene. The reaction mixture was cooled with ice bath and an ice-cold solution of 3,4,5-trimethoxybenzaldehyde (6.13 g, 31.25 mmol) in dry THF (20 ml) was then cannulated to the stirring solution. The resulting reaction mixture was

stirred at 0 °C for 15 min and then brought up to room temperature. The reaction was quenched by adding cold saturated NH_4Cl solution (20 ml). The organic layer was washed with brine and dried over anhydrous $MgSO_4$. The solvent was removed on a rotary evaporator under reduced pressure to afford the crude compound. The crude product was further purified by silica gel column chromatography using EA/Hexanes (3:7) as eluent to collect desired diol (8) as yellow solid (2.91 g, 49%). ^{1}H NMR (400 MHz, $CDCl_3$) δ: 2.57 (s, 1H, OH), 2.58 (s, 1H, OH), 3.83 (s, 18H, OCH_3), 5.89 (d, 2H, *J* =3.48 Hz; *meso*), 6.61 (s, 4H, Ph), 6.71 (d, *J* = 3.36 Hz, 2H, *β*-thiophene) ppm; ^{13}C NMR (100 MHz, $CDCl_3$) δ: 56.12, 60.81, 72.59, 103.28, 103.30, 103.84, 124.39, 124.43, 137.60, 138.50, 147.88, 147.97, 153.27 ppm.

2,5-Bis(*p*-tolylmethanol)thiophene (9): Anhydrous hexane (40 ml) was added to a 250 ml three-necked round-bottomed flask equipped with rubber septum, gas inlet and gas outlet tube. A positive pressure of N_2 was maintained and after purging N_2 gas for 5 min, TMEDA (10.6 ml, 71 mmol) and *n*-BuLi (45 ml of 1.6 M solution in hexane) were added sequentially to the stirring solution at room temperature. Thiophene (1.9 ml, 23.7 mmol) was then added and the solution was refluxed for 1 h. As the reaction progressed, a white turbid solution formed indicating the formation of the 2,5-dilithiated salt of thiophene. The reaction mixture was cooled with ice bath and an ice-cold solution of *p*-tolaldehyde (7 ml, 59.25 mmol) in dry THF (50 ml) was then cannulated to the stirring solution. The resulting reaction mixture was stirred at 0 °C for 15 min and then brought up to room temperature. The reaction was quenched by adding cold saturated NH_4Cl solution (50 ml). The organic layer was washed with brine and dried over anhydrous $MgSO_4$. The solvent was removed on a rotary evaporator under reduced pressure to afford the crude compound. The crude product was further purified by silica gel column chromatography using EA/Hexanes (3:7) as eluent to collect desired diol (9) as yellow solid (6 g, 78%). ^{1}H NMR (400 MHz, $CDCl_3$) δ: 2.35 (s, 6H, CH_3), 2.38 (s, 1H, OH), 2.39 (s, 1H, OH), 5.92 (d, 2H, *J* = 3.60 Hz, *meso*), 6.69 (d, *J* =2.6 Hz, 2H, *β*-thiophene), 7.16 (d, *J* = 7.92 Hz, 4H, *m*-tolyl), 7.30 (d, *J* = 6.84 Hz, 4H, *o*-tolyl) ppm. ^{13}C NMR (100 MHz, $CDCl_3$) δ: 21.13, 72.42, 124.28, 126.22, 129.18, 137.73, 139.99, 148.19 ppm.

Dimethyl 4,4'-(thiophene-2,5-diylbis(hydroxymethylene)) dibenzoate (10): Anhydrous hexane (40 ml) was added to a 250 ml three-necked round-bottomed flask equipped with rubber septum, gas inlet and gas outlet tube. A positive pressure of N_2 was maintained and after purging N_2 gas for 5 min, TMEDA (4.7 ml, 31.25 mmol) and *n*-BuLi (20 ml of 1.6 M solution in hexane) were added sequentially to the stirring solution at room temperature. Thiophene (1 ml, 12.5 mmol) was then added and the solution was refluxed for 1 h. As the reaction progressed, a white turbid solution formed indicating the formation of the 2,5-dilithiated salt of thiophene. The reaction mixture was cooled with ice bath and an ice-cold solution of methyl-4-formylbenzoate (4 g, 25 mmol) in dry THF (20 ml) was then cannulated to the stirring solution. The resulting reaction mixture was stirred at 0 °C for 15 min and then brought up to room temperature. The reaction was quenched by adding cold saturated NH_4Cl solution (20 ml). The organic layer was washed with brine and dried over anhydrous $MgSO_4$. The solvent was removed on a rotary evaporator under reduced pressure to afford the crude compound. The crude product was further purified by silica gel column chromatography using EA/Hexanes (3:7) as eluent to collect desired diol (10) as yellow solid (4.3 g, 84%). ^{1}H NMR (400 MHz, $CDCl_3$) δ: 2.55 (s, 1H, OH), 2.56 (s, 1H, OH), 3.9 (s, 6H, $COOCH_3$), 6.01 (d, 2H, *J* = 3.72 Hz; *meso*), 6.72 (s, 2H, *β*-thiophene), 7.49 (m, 4H, Ph), 8.01 (d, *J* =8.28 Hz, Ph) ppm. ^{13}C NMR (100 MHz, $CDCl_3$) δ: 52.14, 71.97, 124.81, 126.12, 129.77, 129.88, 147.52, 147.74, 166.79.

N3S-2EOMe (11): In a 250 ml one-necked round-bottomed flask fitted with a N_2 gas bubbler, a solution of the thiophene diol (8) (476 mg, 1 mmol), pyrrole (205 µl, 3 mmol) and methyl-4-formylbenzoate (328 mg, 2 mmol) in DCM (200 ml) was taken. Resulting reaction mixture was purged with N_2 for 15 min and then a catalytic amount of BF_3•OEt_2 (15 µl, 0.1 mmol) was added at room temperature. After stirring for 1 h, DDQ (681 mg, 3 mmol) was added and the reaction mixture was stirred at room temperature in air for 1 h. The solvent was removed on a rotary evaporator. The crude product was purified by silica gel column chromatography using Hexanes/DCM (1:1) as eluent to afford the desired porphyrin (11) as purple solid. (379 mg, 20%). ^{1}H NMR (400 MHz, $CDCl_3$) δ: −2.69 (s, 1H, NH), 4.02 (s, 12H, OCH_3), 4.12 (s, 6H, OCH_3), 4.18 (s, 6H, OMe), 7.49 (s, 4H, Ph), 8.28 (d, 4H, *J* = 8.16 Hz; *o*-Ph), 8.45 (d, 4H, *J* = 8.16 Hz; *m*-Ph), 8.56 (d, 2H, *J* = 4.60 Hz; *β*-pyrrole), 8.80 (d, 2H, *J* = 4.48 Hz; *β*-pyrrole), 8.89 (d, 2H, *J* = 1.72 Hz; *β*-pyrrole), 9.87 (s, 2H, *β*-thiophene) ppm; ^{13}C NMR (100 MHz, $CDCl_3$) δ: 52.45, 56.46, 61.27, 112.22, 12.45, 127.91, 128.76, 129.89, 131.80, 133.62, 134.31, 134.69, 135.17, 136.24, 138.19, 138.38, 147.00, 147.55, 152.31, 154.05, 157.52, 167.19 ppm; HRMS-ESI: *m/z* calcd for $C_{54}H_{46}N_3O_{10}S$: 928.2904, found 928.2901 $[M+H]^+$.

N3S-2Etol (12): In a 250 mL one-necked round-bottomed flask fitted with a N_2 gas bubbler, a solution of the thiophene diol (9) (500 mg, 1.54 mmol), pyrrole (316 µl, 4.62 mmol) and methyl-4-formylbenzoate (506 mg, 3.08 mmol) in DCM (200 ml) was taken. Resulting reaction mixture was purged with N_2 for 15 min and then a catalytic amount of BF_3•OEt_2 (20 µl, 0.15 mmol) was added at room temperature. After stirring for 1 h, DDQ (699 mg, 3.08 mmol) was added and the reaction mixture was stirred at room temperature in air for 1 h. The solvent was removed on a rotary evaporator. The crude product was purified by silica gel column chromatography using Hexanes/DCM (1:1) as eluent to afford the desired porphyrin (12) as purple solid. (268 mg, 22%). ^{1}H NMR (400 MHz, $CDCl_3$) δ: −2.70 (s, 1H, NH), 2.72 (s, 6H, CH_3), 4.12 (s, 6H, OMe), 7.64 (d, 4H, *J* = 7.76 Hz; *m*-tolyl), 8.15 (d, 4H, *J* = 7.76 Hz; *o*-tolyl), 8.29 (d, 4H, *J* = 8.08 Hz; *o*-Ph), 8.44 (d, 4H, *J* = 8.04 Hz; *m*-Ph), 8.55

(d, 2H, J = 4.60 Hz; β-pyrrole), 8.74 (d, 2H, J = 4.52 Hz; β-pyrrole), 8.89 (d, 2H, J = 1.4 Hz; β-pyrrole), 9.81 (s, 2H, β-thiophene) ppm. ^{13}C NMR (100 MHz, $CDCl_3$) δ: 21.49, 52.42, 122.03, 127.85, 128.35, 128.60, 129.76, 132.15, 133.73, 134.20, 134.34, 134.73, 134.96, 137.77, 137.88, 138.26, 147.19, 147.68, 153.94, 157.64, 167.24 ppm. HRMS-ESI: *m/z* calcd for $C_{50}H_{38}N_3O_4S$: 776.2583, found 776.2584 $[M+H]^+$.

N3S-2ETPA (13): In a 250 ml one-necked round-bottomed flask fitted with a N_2 gas bubbler, a solution of the thiophene diol (10) (413 mg, 1 mmol), pyrrole (205 µl, 3 mmol) and 4-(diphenylamino)benzaldehyde (546 mg, 2 mmol) in DCM (200 ml) was taken. Resulting reaction mixture was purged with N_2 for 15 min and then a catalytic amount of BF_3•OEt_2 (38 µl, 0.3 mmol) was added at room temperature. After stirring for 1 h, DDQ (681 mg, 3 mmol) was added and the reaction mixture was stirred at room temperature in air for 1 h. The solvent was removed on a rotary evaporator. The crude product was purified by silica gel column chromatography using Hexanes/DCM (1:1) as eluent to afford the desired porphyrin (13) as purple solid. (80 mg, 7%). ^{1}H NMR (400 MHz, $CDCl_3$) δ: −2.59 (s, 1H, NH), 4.12 (s, 6H, OMe), 7.15 (m, 4H, Ph), 7.42 (m, 20H, Ph), 8.05 (d, 4H, J = 8.44 Hz; Ph), 8.34 (d, 4H, J = 8.20 Hz; Ph), 8.50 (d, 4H, J = 8.24 Hz; Ph), 8.64 (d, 2H, J = 4.60 Hz; β-pyrrole), 8.77 (d, 2H, J = 4.64 Hz; β-pyrrole), 9.13 (d, 2H, J = 1.76 Hz; β-pyrrole), 9.67 (s, 2H, β-thiophene) ppm. ^{13}C NMR (100 MHz, $CDCl_3$) δ: 52.44, 120.98, 123.47, 124.7, 125.03, 128.76, 129.19, 129.54, 129.67, 129.86, 132.59, 134.02, 134.18, 135.52, 135.83, 135.97, 145.71, 146.54, 147.74, 147.83, 154.68, 156.85, 167.30. HRMS-FAB+: *m/z* calcd for $C_{72}H_{52}N_5O_4S$: 1082.3740, found 1082.3738 $[M+H]^+$.

N3S-2AOMe: Thiaporphyrin ester (11) (50 mg, 54 mmol) was dissolved in 40 ml THF. To this mixture, 20 equivalent of KOH mixed in 2 ml water was added and the reaction mixture was refluxed for 12 h. After cooling, the organic solvent was removed under pressure. An amount of 20 ml water was added to the reaction mixture and the solution was treated slowly with 1 N HCl. The precipitation formed were filtered off and washed with distilled water. The residue remained is dissolved in methanol and dried in vacuum to yield desired porphyrin as purple solid (48 mg, 98%). ^{1}H NMR (400 MHz, DMSO-*d*6) δ: −2.82 (s, 1H, NH), 3.96 (s, 12H, OCH_3), 3.99 (s, 6H, OCH_3), 7.56 (s, 4H, Ph), 8.33 (d, 4H, J = 8.16 Hz; *o*-Ph), 8.39 (d, 4H, J = 8.24 Hz; *m*-Ph), 8.52 (d, 2H, J = 4.64 Hz; β-pyrrole), 8.80 (d, 2H, J = 4.48 Hz; β-pyrrole), 8.96 (d, 2H, J = 2.04 Hz; β-pyrrole), 9.95 (s, 2H, β-thiophene) ppm. ^{13}C NMR (100 MHz, DMSO-*d*6) δ: 56.26, 60.38, 112.24, 122.39, 127.81, 129.22, 130.67, 131.69, 133.94, 134.19, 135.29, 135.40, 137.62, 145.82, 146.65, 152.09, 153.33, 156.83, 167.42 ppm; IR (Neat): 3327, 2923, 2853, 1711, 1684, 1603, 1582, 1502, 1462, 1406, 1336, 1234, 1122, 942, 792, 715; UV-Vis (THF) λ_{max}/nm (ε/10^3 M^{-1} cm^{-1}) = 431 (438), 513 (39), 549 (14), 625 (5), 679 (8); HRMS-ESI: *m/z* calcd for $C_{54}H_{42}N_3O_{10}S$: 900.2591, found 900.2585 $[M+H]^+$.

N3S-2Atol: N3S-2Etol (12) (250 mg, 0.32 mmol) was dissolved in 60 ml THF. To this mixture, 20 equivalent of KOH mixed in 10 ml water was added and the reaction mixture was refluxed for 12 h. After cooling, the organic solvent was removed under pressure. An amount of 50 mL water was added to the reaction mixture and the solution was treated slowly with 1 N HCl. The precipitation formed were filtered off and washed with distilled water. The residue remained is dissolved in methanol and dried in vacuum to yield porphyrin as purple solid (215 mg, 90%). ^{1}H NMR (400 MHz, DMSO-*d*6) δ: −2.87 (s, 1H, NH), 2.67 (s, 6H, CH_3), 7.70 (d, 4H, J = 7.60 Hz; *m*-tolyl), 8.14 (d, 4H, J = 7. 64 Hz; *o*-tolyl), 8.33 (d, 4H, J = 8.04 Hz; *o*-Ph), 8.38 (d, 4H, J = 8.04 Hz; *m*-Ph), 8.52 (d, 2H, J = 4.64 Hz; β-pyrrole), 8.67 (d, 2H, J = 4.60 Hz; β-pyrrole), 8.97 (d, 2H, J = 1.84 Hz; β-pyrrole), 9.81 (s, 2H, β-thiophene) ppm. ^{13}C NMR (100 MHz, DMSO-*d*6) δ: 21.03, 122.29, 124.89, 127.78, 128.59, 129.28, 130.68, 131.78, 133.69, 133.93, 134.23, 135.08, 135.33, 137.04, 137.67, 145.79, 146.60, 153.31, 156.77, 167.41 ppm; IR (Neat): 3325, 2920, 2854, 1732, 1686, 1608, 1420, 1313, 1282, 967, 795, 710; UV-vis (THF) λ_{max}/nm (ε/10^3 $M^{-1}cm^{-1}$) = 428 (369), 512 (28), 547 (8), 624 (2), 679 (6); HRMS-ESI: *m/z* calcd for $C_{48}H_{34}N_3O_4S$: 748.2270, found 748.2267 $[M+H]^+$.

N3S-2ATPA: Thiaporphyrin ester (13) (50 mg, 46 mmol) was dissolved in 30 ml THF. To this solution, 20 equivalent of KOH mixed in 2 ml water was added and the reaction mixture was refluxed for 12 h. After cooling, the organic solvent was removed under pressure. An amount of 20 mL water was added to the reaction mixture and was treated slowly with 1 N HCl. The precipitation formed were filtered off and washed with distilled water. The residue remained is dissolved in methanol and dried in vacuum to yield desired porphyrin as purple solid (48 mg, 98%). ^{1}H NMR (400 MHz, DMSO-*d*6) δ: −2.72 (s, 1H, NH), 7.19 (m, 4H, Ph), 7.37 (m, 12H, Ph), 7.47 (m, 8H, Ph), 8.08 (d, 4H, J = 8.20 Hz; Ph), 8.36 (d, 4H, J = 8.00 Hz; Ph), 8.44 (d, 4H, J = 8.04 Hz; Ph), 8.64 (d, 2H, J = 4.44 Hz; β-pyrrole), 8.71 (d, 2H, J = 4.52 Hz; β-pyrrole), 9.15 (s, 2H, β-pyrrole), 9.74 (s, 2H, β-thiophene), 13.30 (br s, 2H, COOH) ppm. ^{13}C NMR (100 MHz, DMSO-*d*6) δ: 120.25, 123.76, 124.40, 124.88, 128.74, 129.50, 129.82, 129.94, 130.45, 132.89, 134.14, 134.78, 135.49, 136.04, 138.62, 144.33, 145.76, 147.08, 147.39, 153.90, 156.20, 167.41 ppm; IR (Neat): 3332, 2918, 2867, 1686, 1590, 1489, 1418, 1313, 1276, 1173, 968, 797, 695; UV-Vis (THF) λ_{max}/nm (ε/10^3 M^{-1} cm^{-1}) = 429 (394), 518 (52), 558 (32), 621 (8), 682 (16); HRMS-ESI: *m/z* calcd for $C_{70}H_{48}N_5O_4S$: 1054.3427, found 1054.3433 $[M+H]^+$.

Photovoltaic Measurements

TiO_2 photoanode films and Pt counter electrodes were purchased from Yingkou Opvtech New Energy Co. Ltd. Liaoning, China. The films, which were prepared by using the screen-printing method, were composed of a transparent layer (thickness ≈ 12 µm), a scattering layer (thickness ≈ 4 µm), and a working area of 0.4×0.4 cm^2 and were used as received. The films were pretreated according to the following activation

procedures before use: heating at 100 ºC for 22 min, at 110 ºC for 60 min, at 450 ºC for 68 min, at 500 ºC 60 min, at 250 ºC for 60 min, cooling at 80 ºC and keeping at 80 ºC before immersion. The TiO_2 films were immersed in a 2×10^{-4} M solution of the porphyrin in THF for 6-8 h at 25 ºC. The dye-sensitized TiO_2 films were washed with THF, dried in hot air, and used as the working electrode. To fabricate the DSSC device, the two electrodes were tightly clipped together into a sandwich-type cell that was spaced by a 40 μm film spacer. A thin layer of electrolyte, which contained 0.05 M I_2, 0.1 M lithium iodide (LiI), 0.6 M dimethyl-propyl-benzimidiazole iodide (DMPII), and 0.6 M 4-tert-butylpyridine (TBP) in dry CH_3CN, was introduced into the space between the two electrodes. The photo-electrochemical characterizations of the solar cells were performed on an Oriel Class A solar simulator (Oriel 91195A, Newport Corp.). Photocurrent–voltage characteristics of the DSSCs were recorded on a potentiostat/galvanostat (CHI650B, CH Instruments, Inc.) at a light intensity of 100 $mWcm^{-2}$ and calibrated to an Oriel reference solar cell (Oriel 91150, Newport Corp.). The monochromatic quantum efficiency was recorded on a monochromator (Oriel 74100, Newport Corp.) under short-circuit conditions. The intensity of each wavelength was within the range 1–3 $mWcm^{-2}$. The EIS measurements were carried on CHI 621B electrochemical impedance analyser (CH Instruments, Austin, TX, USA), under applied AC voltage and bias potential on the cells and measured the corresponding current and voltage under the white LED lamp with various neutral density filters for white light intensity in order to change the Fermi level of DSSCs. The data was analysed using Zview software.

Acknowledgements

The authors greatly acknowledge financial support from the National Science Council (Taiwan) and the Academia Sinica. Mass spectroscopy analysis was performed by the Mass Spectrometry Facility of the Institute of Chemistry, Academia Sinica (Taiwan). Help from Dr. Jiann-T'suen Lin with the measurements and instrumentation is greatly appreciated.

Notes and references

[a] Institute of Chemistry, Academia Sinica, Nankang Taipei, 115 Taiwan.
[b] Department of Chemistry, National Taiwan Normal University, Taipei, 116 Taiwan.

Electronic Supplementary Information (ESI) available: [ATR-FTIR for N3S-ECA, N3S-ECN, N3S-2AOMe and N3S-2ATPA; ^1H, ^{13}C NMR and HR-Mass spectra of thiaporphyrins]. See DOI: 10.1039/b000000x/

1. B. O'Regan and M. Gratzel, *Nature*, 1991, **353**, 737-740.
2. L. M. Goncalves, V. de Zea Bermudez, H. A. Ribeiro and A. M. Mendes, *Energy Environ. Sci.*, 2008, **1**, 655-667.
3. L. Han, A. Islam, H. Chen, C. Malapaka, B. Chiranjeevi, S. Zhang, X. Yang and M. Yanagida, *Energy Environ. Sci.*, 2012, **5**, 6057-6060.
4. W. M. Campbell, K. W. Jolley, P. Wagner, K. Wagner, P. J. Walsh, K. C. Gordon, L. Schmidt-Mende, M. K. Nazeeruddin, Q. Wang, M. Grätzel and D. L. Officer, *J. Phys. Chem. C*, 2007, **111**, 11760-11762.
5. T. Bessho, S. M. Zakeeruddin, C.-Y. Yeh, E. W.-G. Diau and M. Grätzel, *Angew. Chem. Int. Ed.*, 2010, **49**, 6646-6649.
6. A. Yella, H.-W. Lee, H. N. Tsao, C. Yi, A. K. Chandiran, M. K. Nazeeruddin, E. W.-G. Diau, C.-Y. Yeh, S. M. Zakeeruddin and M. Grätzel, *Science*, 2011, **334**, 629-634.
7. A. Hagfeldt, G. Boschloo, L. Sun, L. Kloo and H. Pettersson, *Chem. Rev.*, 2010, **110**, 6595-6663.
8. H. Imahori, T. Umeyama and S. Ito, *Acc. Chem. Res.*, 2009, **42**, 1809-1818.
9. L.-L. Li and E. W.-G. Diau, *Chem. Soc. Rev.*, 2013, **42**, 291-304.
10. M. V. Martinez-Diaz, G. de la Torre and T. Torres, *Chem. Commun.*, 2010, **46**, 7090-7108.
11. P. J. Chmielewski and L. Latos-Grażyński, *Coord. Chem. Rev.*, 2005, **249**, 2510-2533.
12. I. Gupta and M. Ravikanth, *Coord. Chem. Rev.*, 2006, **250**, 468-518.
13. J.-H. Ha, S. Ko, C.-H. Lee, W.-y. Lee and Y.-R. Kim, *Chem. Phys. Lett.*, 2001, **349**, 271-278.
14. P. Ziółkowski, K. Symonowicz, P. Chmielewski, L. Latos-Grażyński, G. Streckyte, R. Rotomskis and J. Rabczyński, *J Cancer Res Clin Oncol*, 1999, **125**, 563-568.
15. D. G. Hilmey, M. Abe, M. I. Nelen, C. E. Stilts, G. A. Baker, S. N. Baker, F. V. Bright, S. R. Davies, S. O. Gollnick, A. R. Oseroff, S. L. Gibson, R. Hilf and M. R. Detty, *J. Med. Chem.*, 2001, **45**, 449-461.
16. R. Minnes, H. Weitman, Y. You, M. R. Detty and B. Ehrenberg, *J. Phys. Chem. B*, 2008, **112**, 3268-3276.
17. E. J. Ngen, T. S. Daniels, R. S. Murthy, M. R. Detty and Y. You, *Bioorg. Med. Chem.*, 2008, **16**, 3171-3183.
18. Y. You, S. L. Gibson, R. Hilf, S. R. Davies, A. R. Oseroff, I. Roy, T. Y. Ohulchanskyy, E. J. Bergey and M. R. Detty, *J. Med. Chem.*, 2003, **46**, 3734-3747.
19. Y. You, S. L. Gibson, R. Hilf, T. Y. Ohulchanskyy and M. R. Detty, *Bioorg. Med. Chem.*, 2005, **13**, 2235-2251.
20. I. Gupta and M. Ravikanth, *J. Org. Chem.*, 2004, **69**, 6796-6811.
21. Y. Pareek and M. Ravikanth, *RSC Advances*, 2014, **4**, 7851-7880.
22. S. Stute, K. Gloe and K. Gloe, *Tetrahedron*, 2005, **61**, 2907-2912.
23. Y. Xie, P. Joshi, M. Ropp, D. Galipeau, L. Zhang, H. Fong, Y. You and Q. Qiao, *J. Porphyrins Phthalocyanines*, 2009, **13**, 903-909.
24. C.-H. Hung, C.-K. Ou, G.-H. Lee and S.-M. Peng, *Inorg. Chem.*, 2001, **40**, 6845-6847.
25. C.-H. Chuang, C.-K. Ou, S.-T. Liu, A. Kumar, W.-M. Ching, P.-C. Chiang, M. A. C. dela Rosa and C.-H. Hung, *Inorg. Chem.*, 2011, **50**, 11947-11957.
26. S. B. Mane, J.-Y. Hu, Y.-C. Chang, L. Luo, E. W.-G. Diau and C.-H. Hung, *Chem. Commun.*, 2013, **49**, 6882-6884.
27. S. B. Mane, L. Luo, G.-F. Chang, E. W.-G. Diau and C.-H. Hung, *J. Chin. Chem. Soc.*, 2014, DOI: 10.1002/jccs.201300525.
28. C.-F. Lo, L. Luo, E. W.-G. Diau, I. J. Chang and C.-Y. Lin, *Chem. Commun.*, 2006, 1430-1432.
29. Y. Arai and H. Segawa, *Chem. Commun.*, 2010, **46**, 4279-4281.
30. R. Ambre, K.-B. Chen, C.-F. Yao, L. Luo, E. W.-G. Diau and C.-H. Hung, *J. Phys. Chem. C*, 2012, **116**, 11907-11916.
31. R. B. Ambre, G.-F. Chang and C.-H. Hung, *Chem. Commun.*, 2014, **50**, 725-727.
32. R. B. Ambre, G.-F. Chang, M. R. Zanwar, C.-F. Yao, E. W.-G. Diau and C.-H. Hung, *Chem. Asian J.*, 2013, **8**, 2144-2153.
33. A. Abbotto, N. Manfredi, C. Marinzi, F. De Angelis, E. Mosconi, J.-H. Yum, Z. Xianxi, M. K. Nazeeruddin and M. Gratzel, *Energy Environ. Sci.*, 2009, **2**, 1094-1101.
34. C.-J. Yang, Y. J. Chang, M. Watanabe, Y.-S. Hon and T. J. Chow, *J. Mater. Chem.*, 2012, **22**, 4040-4049.
35. M. J. Frisch, Gaussian 09, Revision A.1, *Gaussian, Inc., Wallingford CT*, 2009.
36. I. Gupta, N. Agarwal and M. Ravikanth, *Eur. J. Org. Chem.*, 2004, **2004**, 1693-1697.
37. S. Punidha, N. Agarwal, R. Burai and M. Ravikanth, *Eur. J. Org. Chem.*, 2004, **2004**, 2223-2230.
38. S. Punidha, N. Agarwal, I. Gupta and M. Ravikanth, *Eur. J. Org. Chem.*, 2007, **2007**, 1168-1175.